Allometric and Metameric Shape Variation in *Pan* Mandibular Molars: A Digital Morphometric Analysis

MICHELLE SINGLETON,[1]* ALFRED L. ROSENBERGER,[2,3] CHRIS ROBINSON,[3,4] AND ROB O'NEILL[5]

[1]Department of Anatomy, Midwestern University, Downers Grove, Illinois
[2]Department of Anthropology & Archaeology, Brooklyn College–CUNY, Brooklyn, New York
[3]New York Consortium in Evolutionary Primatology
[4]Department of Biology & Medical Lab Technology, Bronx Community College–CUNY, Bronx, New York
[5]Department of Digital Arts, Digital Arts Research Lab, Pratt Institute, New York, New York

ABSTRACT

The predominance of molar teeth in fossil hominin assemblages makes the patterning of molar shape variation a topic of bioanthropological interest. Extant models are the principal basis for understanding dental variation in the fossil record. As the sister taxon to the hominin clade, *Pan* is one such model and the only widely accepted extant hominid model for both interspecific and intraspecific variation. To explore the contributions of allometric scaling and meristic variation to molar variation in *Pan*, we applied geometric shape analysis to 3D landmarks collected from virtual replicas of chimpanzee and bonobo mandibular molars. Multivariate statistical analysis and 3D visualization of metameric and allometric shape vectors were used to characterize shape differences and test the hypothesis that species of *Pan* share patterns of metameric variation and molar shape allometry. Procrustes-based shape variables were found to effectively characterize crown shape, sorting molars into species and tooth-row positions with $\geq$95% accuracy. Chimpanzees and bonobos share a common pattern of M_1–M_2 metameric variation, which is defined by differences in the relative position of the metaconid, size of the hypoconulid, curvature of the buccal wall, and proportions of the basins and foveae. Allometric scaling of molar shape is homogeneous for M_1 and M_2 within species, but bonobo and chimpanzee allometric vectors are significantly different. Nevertheless, the common allometric shape trend explains most molar-shape differences between *P. paniscus* and *P. troglodytes*. When allometric effects are factored out, chimpanzee and bonobo molars are not morphometrically distinguishable. Implications for hominid taxonomy and dietary reconstruction are discussed. Anat Rec, 294:322–334, 2011. © 2010 Wiley-Liss, Inc.

Key words: chimpanzee; bonobo; allometry; meristic variation; digital morphology

Additional Supporting Information may be found in the online version of this article.

Grant sponsor: The Leakey Foundation.

*Correspondence to: Michelle Singleton, Anatomy Department, Midwestern University, 555 31st Street, Downers Grove, IL 60515. Fax: 630-515-7199. E-mail: msingl@midwestern.edu

Received 19 November 2009; Accepted 19 August 2010
DOI 10.1002/ar.21315
Published online 22 December 2010 in Wiley Online Library (wileyonlinelibrary.com).

Postcanine teeth, by virtue of their extreme durability, comprise a significant proportion of the human fossil record, and isolated molars make up the greater part of many hominin assemblages (Leakey et al., 1976; Johanson et al., 1982; Leakey et al., 1995; Suwa et al., 1996; Leakey et al., 1998; Braga and Thackeray, 2003). Because molar morphology features prominently in hominin species descriptions as well as in assessments of hominin evolutionary relationships and ecology, molar shape variation is a topic of some practical concern (Leakey et al., 1976; White et al., 1981; Leakey et al., 1995; Brunet et al., 1996; Suwa et al., 2007).

As the sister taxon to the hominin clade, *Pan* occupies a pivotal position in discussions of hominid molar diversity (e.g., Corruccini and McHenry, 1979; McHenry and Corruccini, 1980, 1981; Uchida, 1996; Scott and Lockwood, 2004; Pilbrow, 2006; Bailey, 2008). On both morphological and phylogenetic grounds, *Pan* is a logical model for early hominin molar shape variation (Corruccini and McHenry, 1979; Hlusko, 2002). It is also the only widely accepted, extant hominid exemplar of both interspecific and intraspecific variation (Bailey, 2008). Although differing in their methodologies, Bailey's (2008) investigation of nonmetric molar trait distributions in *Pan* and Pilbrow's (2006) analysis of chimpanzee molar morphometrics share with earlier studies (e.g., Corruccini and McHenry, 1979; Hlusko, 2002) the fundamental premise that a deeper understanding of molar shape variation within and between species of *Pan* can help explicate patterns observed in the hominin fossil record (Pilbrow, 2006; Bailey, 2008).

Although morphological studies generally concur that molar shape differences reflect phylogenetic relationships within and between species of *Pan* (Corruccini and McHenry, 1979; McHenry and Corruccini, 1981; Uchida, 1996; Pilbrow, 2006), they disagree on important points, such as the contribution of allometry. For example, Pilbrow's (2006) multivariate analysis of occlusal dimensions and cusp areas revealed a strong correspondence between molar morphology and genetic distances among taxa; her discriminant function analyses classified molars to subspecies with up to 77% accuracy and to species with 73–96% accuracy. However, morphometric separation among taxa and classification accuracy dropped off markedly when variables were scaled by the geometric mean, a sign that classifications were driven by size. This result led her to conclude that at least some molar dimensions are "ontogenetically scaled" (Pilbrow, 2006: 655) in chimpanzees and bonobos and that "primarily molar size rather than shape distinguish(es) the two species" (Pilbrow, 2006: 654).

Although differences in absolute molar size between chimpanzees and bonobos unquestionably exist (Coolidge, 1933; Remane, 1962; Johanson, 1974a; McHenry and Corruccini, 1981; Shea, 1982; Kinzey, 1984; Uchida, 1996), Pilbrow's conclusion requires clarification in light of her methods. Whereas Mosimann shape indices (e.g., linear dimensions scaled by the geometric mean) correct for differences in absolute size (scale), they do not eliminate allometric differences in relative proportion (shape) (Mosimann and Malley, 1979). So, it may not be simply size, *per se*, but allometric shape differences that distinguish populations of *Pan*. This alternative is implicit in Pilbrow's invocation of scaling.

Whereas a number of prior studies have examined the scaling of hominid molar size relative to cranial size (Pilbeam and Gould, 1975; Shea, 1981, 1982, 1983, 1984), only a few have addressed molar shape allometry in its own right (Corruccini and McHenry, 1979; McHenry and Corruccini, 1981; Uchida, 1996). Corruccini and McHenry recognized the molar dentition as "the system in which *Pan* species differ most" (1979: 1342) and found a relatively low correlation (−0.37) between interspecific and intraspecific vectors of molar allometry. Differences between bonobos and chimpanzees in molar crown shape, cusp proportion, and talonid height were therefore not, in their opinion, attributable to scaling. Kinzey (1984) also questioned the contribution of allometry to interspecific shape differences. This lack of consensus on the role of allometry hinders interpretation of molar shape differences between chimpanzees and bonobos. Given the intrinsic importance of hominid dental variation and its relevance to paleoanthropological interpretation, the nature of molar-shape allometry in *Pan* merits further scrutiny.

If allometric shape variation is a pervasive influence on primate morphology, metameric (meristic) variation—shape differences between serially homologous morphological elements such as vertebrae and molars (Bateson, 1894; Hlusko, 2002)—is a more limited and less well-understood phenomenon. Such differences are often subtle (Polly and Head, 2004), and the risk of conflating metameric and taxonomic variation is a general concern (Hlusko, 2002). Hlusko's analysis of meristic variation in hominid mandibular molars identified a shared African-ape pattern characterized by differences in the buccal wall contour (M_2 more curved) and the proportions of the mesial fovea (expanded in M_2) and distobuccal crown (compressed in M_2). Because her study did not include *P. paniscus*, the nature of bonobo meristic variation remains an open question. Given Hlusko's conclusion that meristic variation in South African australopiths more closely resembles the African-ape pattern than that of modern *Homo*, a more complete characterization of meristic variation within *Pan* is also warranted.

Geometric morphometric (GM) analyses of skeletal—and particularly cranial—morphology are routinely used to investigate hominid taxonomy, evolutionary relationships, and development (Bookstein et al., 1999; Delson et al., 2001; Ponce de Leon and Zollikover, 2001; Ackermann and Krovitz, 2002; Lockwood et al., 2002; Bookstein et al., 2003; Robinson, 2003; Berge and Penin, 2004; Harvati, 2004; Harvati et al., 2004; Lockwood et al., 2004; Mitteroecker et al., 2004; Cobb and O'Higgins, 2007; Slice, 2007; Baab and McNulty, 2009). By contrast, GM studies of hominid dental shape are comparatively few and are notable for their sparse landmark sampling and essentially 2D approach, analyzing occlusal surfaces and outlines or crown profiles but seldom both simultaneously (Ungar et al., 1994; McNulty et al., 1999; Hlusko, 2002; Olejniczak et al., 2004; Martinón-Torres et al., 2006; Bailey and Wood, 2007; Gómez-Robles et al., 2007, 2008; White, 2009). Boughner and Dean's (2004) study of molar-crown initiation used 3D molar landmarks but did not deal specifically with molar-shape variation. To our knowledge, Skinner and colleagues (Skinner et al., 2008, 2009b) are the only researchers to have used 3D GM methods to analyze hominid molars, specifically the enamel-dentine junction (EDJ), which they found to discriminate between species and subspecies of *Pan* and between *Australopithecus* and *Paranthropus*.

TABLE 1. Study sample

	Abbr.	M_1	M_2	Source
Pan paniscus	Ppn	13	12	RMCA*
Pan troglodytes	Ptx	8	11	HPM, CSHO

*Dental molds of *Pan paniscus* were produced by Peter Ungar and used with his consent.
CSHO = Daris R. Swindler Collection, Center for the Study of Human Origins, New York University.
HPM = Peabody Museum of Archaeology and Ethnology, Harvard University.
RMCA = Royal Museum for Central Africa.

In the present study, 3D GM methods were used to test the hypothesis that species of *Pan* share common patterns of metameric variation and molar shape allometry. Three-dimensional landmarks were collected from high-resolution digital models of chimpanzee and bonobo mandibular molars to capture the shape of the entire crown, including buccal and lingual walls. Multivariate statistical analysis and 3D visualization were used to characterize shape trends within and across species; random permutation tests were applied to determine the statistical significance of interspecific differences in metameric and allometric patterning. Through this investigation, we sought to resolve several interrelated questions: (1) Do chimpanzees and bonobos share a common pattern of metameric shape variation? (2) Do first and second mandibular molars share common allometric scaling patterns within species? (3) Is molar shape allometrically scaled in chimpanzees and bonobos? (4) If so, does allometry fully account for interspecific differences, or are some differences independent of molar size? The answers to these longstanding questions may bear on our interpretations of extant and fossil hominid molar variation.

MATERIAL AND METHODS

Data

Materials. Table 1 lists the specimens used in this study. The sample comprises first and second mandibular molars of *Pan troglodytes* and *Pan paniscus*. Sexual dimorphism in molar dimensions and relative cusp proportions is low or absent in *Pan* (Johanson, 1974b; Uchida, 1996), therefore, no effort was made to control for the sample's sex composition. Although potentially increasing within-sample shape variation, between-sex differences are not of sufficient magnitude to obscure the larger between-element and between-species shape differences that were the focus of this study. Specimens were chosen on the basis of completeness and wear, which was scored on a 10-point scale with 0 indicating absence of wear and 10 signifying dental senescence (Benefit, 1993). In our sample, molars of *P. troglodytes* were more worn, on average, than those of *P. paniscus*, with median wear scores of 4 and 2, respectively. Within species, M_1 and M_2 scores differed by 1–2 points. Molars of *P. troglodytes verus* from the Peabody Museum of Archaeology and Ethnology (Harvard) were molded using President Jet^{TM} Medium Body vinyl polysiloxane impression material (Coltène/Whaledent) following standard protocols (Ungar, 1996; Ungar and Williamson, 2000). Existing molds of bonobo molars produced by Peter Ungar were provided by the Royal Museum for Central Africa (Tervuren, Belgium) with his consent. High-resolution, epoxy casts were prepared using F-82 Epoxy Resin (Eastpointe Fiberglass, Eastpointe, MI). Dimensionally accurate, dental-stone casts of *P. troglodytes troglodytes* from the Daris R. Swindler Collection (Center for the Study of Human Origins, New York University) were also included in this study (Swindler et al., 1963). Differences in fidelity between these two casting materials were not expected to influence results because the tolerances of the respective media are less than the error associated with the landmark collection procedure (see Electronic Supporting Information; Swindler et al., 1963; Ungar, 1996).

Data acquisition and processing. Molar casts were laser scanned using an LDI Surveyor AM-66RR laser digitizer (Laser Design) equipped with an RPS-120 sensor set to maximum point density (0.025 mm). Where possible, the entire crown surface (excluding interproximal surfaces) was scanned, but in some cases the cemento-enamel junction and/or lower crown walls were obscured (e.g., by high clay lines) or absent (Swindler dental plaques). To correct for their slight translucence, epoxy casts were coated with a thin, matte layer of water-based paint before scanning.

Raw point clouds were filtered, surface-rendered, and trimmed using *Geomagic Studio* (Raindrop Geomagic) to create 3D digital replicas of individual molar crowns. Scans of left molars were mirror imaged to permit direct shape comparisons among all specimens. Three-dimensional landmarks (Fig. 1) were placed using Landmark 3.0.0.6, a data acquisition tool specifically created for 3D geometric applications (Wiley et al., 2005). Following previous landmark-based studies (Wood et al., 1983; Hartman, 1989; Ungar et al., 1994; Hlusko, 2002), landmarks were chosen to record the locations of cusp apices, depressions, fissure intersections, and maxima of crown-wall curvature (Table 2). A subset of eight landmarks, selected to encompass the crown's mesiodistal, buccolingual, and cervico-apical dimensions, was used to define correspondences between each sample specimen and a template specimen or atlas (Table 2, Fig. 1). These correspondences guided the automated transfer of the entire landmark set to the target specimen. Landmarks were then adjusted manually to achieve accurate positioning; where a landmark's true position was absent or could not be confidently identified (e.g., at the CEJ), that landmark was classified as missing. Reliability studies showed this protocol to have maximum intra- and inter-observer errors of $<5\%$ across all landmarks (see Electronic Supporting Information).

Generalized Procrustes analysis (GPA) performed in *Morpheus* (Slice, 1998) was used to optimally align molar landmark configurations in a common shape space (Gower, 1975; Rohlf and Slice, 1990; Dryden and Mardia, 1998). Following alignment, coordinates for missing landmarks were estimated using thin-plate spline (TPS) estimation (Bookstein, 1991; Gunz, 2005; Gunz et al., 2009). In this approach, a thin-plate spline interpolation is computed between an incomplete specimen (target) and a complete reference configuration such as the Procrustes consensus using landmarks common to both. Missing target landmarks are then estimated by

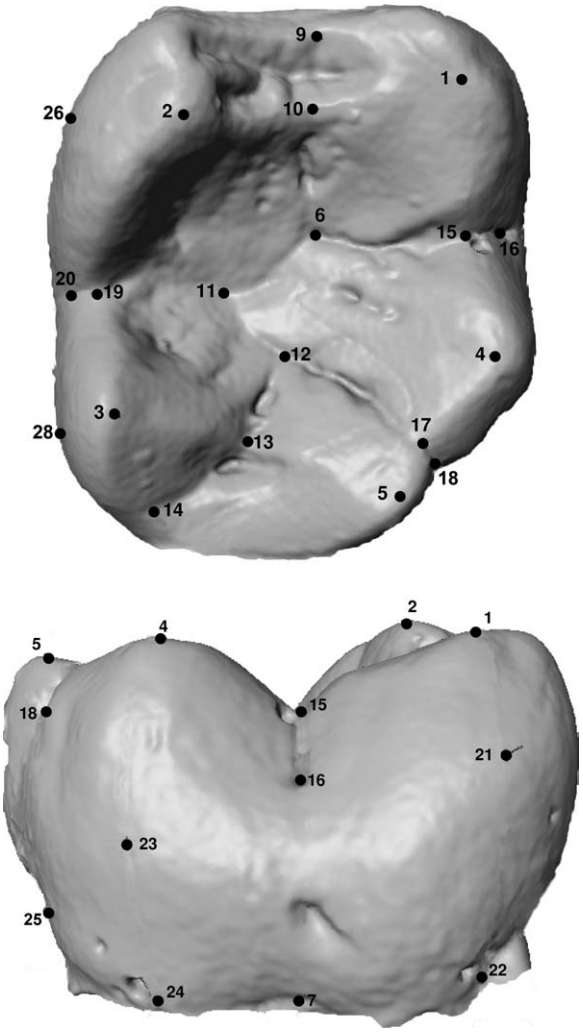

Fig. 1. Three-dimensional landmarks. Landmarks are shown positioned on the atlas specimen, a bonobo right M_1, shown here in occlusal (top) and buccal (bottom) views. Landmark numbers correspond to Table 2; landmarks 8, 27, and 29 are not shown.

application of the TPS interpolation function to the homologous reference landmarks (Gunz, 2005; Gunz et al., 2009). Accordingly, a Procrustes consensus was calculated for each species-molar group (e.g., *P. paniscus*–M_1), and each incomplete specimen was mapped to its group reference using all landmarks present in that specimen. Across the entire sample, 36 of 1,276 landmarks (2.8%) were estimated. For reasons noted above, the majority of these were cervical landmarks.

Analysis

The statistical significance of molar shape differences within and between species was tested by random permutation of Procrustes distances between mean shapes. Procrustes distance (ρ) is the Euclidean distance in shape space between two optimally aligned landmark configurations (Bookstein, 1991; Slice et al., 1996). For each comparison, individuals were randomized with respect to group (either molar position or species), and the Procrustes distance between the permuted group means was calculated. This sequence was repeated 1,000 times, and shapes were considered significantly different if the observed distance exceeded 95% of the permuted distances (Good, 2000; Zelditch et al., 2004).

Principal components analysis (PCA) of the covariance matrix of the Procrustes-aligned coordinates was used to ordinate specimens in a reduced-dimension morphospace, yielding a matrix of independent variables, the principal shape component (SPC) scores, which summarize the majority of sample shape variation (Dryden and Mardia, 1998). These variables were carried through to subsequent statistical analyses. Discriminant function analysis (DFA) was used to assess the ability of crown shape to accurately classify molars to species and molar-row position. Two-way analysis of variance (ANOVA) of SPC scores was used to evaluate the relative contribution of differential wear to shape differences between first and second molars and between species. To account for the unbalanced design and presence of empty cells, Type IV sums of squares (vs. the usual Type III) were employed (Goodnight, 1978; SAS, 1990); in each case, Levene's (1960) test confirmed homogeneity of variance for the principal effect. Thin-plate spline estimation and statistical analyses were performed in SAS 9.13 (SAS Institute, Cary, NC). Procrustes distance calculations and permutation tests were executed using Interactive Matrix Language (IML) modules adapted from SAS routines written by Kieran McNulty (McNulty, 2005a,b).

Metameric shape variation. Differences in metameric variation patterns between species of *Pan* were examined using two-way analysis of variance (ANOVA) of principal shape component scores. A significant interaction between species and molar-position effects indicates significant differences in metameric patterning between chimpanzees and bonobos (Zelditch et al., 2004). Metameric variation was also examined by direct comparison of metameric shape vectors. The metameric vector for each species is the coefficient vector derived by regression of its aligned-coordinate matrix on a two-state categorical (dummy) variable representing molar-row position (Zelditch et al., 2004; Collyer and Adams, 2007). Differences in the orientation of metameric vectors were measured as the angle between them, which is calculated as the arccosine of the vector correlation (dot product) (Klingenberg, 1996; Zelditch et al., 2004; Collyer and Adams, 2007). Differences in vector magnitude were measured as the absolute difference in vector lengths, where the length of the metameric vector $\mathbf{M}$ is $|\mathbf{M}| = \mathbf{M}^*\mathbf{M}'$.

Random permutation tests were used to determine the statistical significance of observed differences in metameric vector orientation and magnitude. The dataset was divided into four partitions: *P. paniscus*/M_1, *P. troglodytes*/M_1, *P. paniscus*/M_2, and *P. troglodytes*/M_2. Equal random samples of $N = 8$ specimens were drawn from each partition, eight being the size of the smallest partition, *P. troglodytes*/M_1. Holding the M_1 and M_2 samples separate, specimens were then randomly reassigned to species, and angular and vector-length differences were computed between the permuted M_1 and M_2 samples. This sequence was repeated for 1,000 iterations. The observed difference was considered significant if it

TABLE 2. Three-dimensional landmarks collected from virtual molar surfaces

#	Class	Landmark	Description
1	Cusp	PCD*	Geometric center of protoconid apex
2	Cusp	MCD*	Geometric center of metaconid apex
3	Cusp	ECD*	Geometric center of entoconid apex
4	Cusp	HCD*	Geometric center of hypoconid apex
5	Cusp	HCLD*	Geometric center of hypoconulid apex
6	Groove	OC3*	Intersection of mesiobuccal groove with the LDG
7	Buccal	BC1*	At CEJ directly inferior to OC8
8	Lingual	LC1*	At CEJ directly inferior to OC12
9	Groove	OC1	Inferior-most point on mesial marginal ridge
10	Groove	OC2	Intersection of LDG with protocristid
11	Groove	OC4	Intersection of distobuccal groove with buccal face of entoconid
12	Groove	OC5	Intersection of lingual groove with lingual face of hypoconid
13	Groove	OC6	Intersection of LDG with distal margin of occlusal table
14	Groove	OC7	Intersection of LDG with the mesial border of the distal fovea
15	Groove	OC8	Intersection of mesiobuccal groove with buccal margin of occlusal table
16	Groove	OC9	Intersection of mesiobuccal groove with buccal wall
17	Groove	OC10	Intersection of distobuccal groove with buccal margin of occlusal table
18	Groove	OC11	Intersection of distobuccal groove with buccal wall
19	Groove	OC12	Intersection of lingual groove with lingual margin of occlusal table
20	Groove	OC13	Intersection of lingual groove with lingual wall
21	Buccal	MBM	Buccal-most point on buccal face directly inferior to PCD
22	Buccal	MBC	At CEJ directly inferior to PCD
23	Buccal	DBM	Buccal-most point on buccal face directly inferior to HCD
24	Buccal	DBC	At CEJ directly inferior to HCD
25	Buccal	BC2	At CEJ directly inferior to O10
26	Lingual	MLM	Lingual-most point on lingual face directly inferior to MCD
27	Lingual	MLC	At CEJ directly inferior to MCD
28	Lingual	DLM	Lingual-most point on lingual face directly inferior to ECD
29	Lingual	DLC	At CEJ directly inferior to ECD

*Correspondence landmark.
LDG, longitudinal developmental groove; CEJ, cemento-enamel junction.

exceeded 95% of the permuted values (Good, 2000; Zelditch et al., 2004).

Allometric shape variation. Because the classic definition of ontogenetic scaling, adult shape difference arising from truncation/extension of a common ontogenetic trajectory (Gould, 1975; Shea, 1982), is not applicable to mature teeth, we followed previous studies in adopting unity of static (adult intraspecific) allometries as our criterion for determining whether chimpanzee and bonobo molars are allometrically scaled (Corruccini and McHenry, 1979; McHenry and Corruccini, 1981). Following Mitteroecker et al. (Mitteroecker et al., 2004), allometric scaling patterns were explored using a principal components analysis in form space, the morphospace constructed by augmenting the matrix of Procrustes-aligned coordinates by a size vector, specifically log centroid size (hereafter simply "size"). A specimen's centroid size is calculated as the square root of summed squared distances of its landmarks to the specimen centroid (Bookstein, 1991; Slice et al., 1996). In a form-space PCA, the first principal component (FPC1) is expected to summarize both geometric size and the common allometric shape trend, both major sources of variance (Mitteroecker et al., 2004). Higher order PCs summarize shape variation that is statistically independent of size (Jolicoeur and Mosimann, 1960; Jolicoeur, 1963; Klingenberg, 1996; Mitteroecker et al., 2004). Differences in scaling within and between species were tested by direct comparison of FPC1 eigenvectors calculated separately for the two species (Jolicoeur, 1963; Klingenberg, 1996). Differences in allometric vector orientation were measured as the angle between vectors, as described above. Random permutation tests were used to determine the statistical significance of observed differences in vector orientation and magnitude. For within-species comparisons, equal random samples (N = 8, *P. troglodytes*; N = 10, *P. paniscus*) of first and second molars were combined and randomly reassigned to molar-row position. For interspecific comparisons, equal random samples (N = 15) of chimpanzee and bonobo molars were combined and randomly reassigned to species. The angular difference was computed for the permuted samples. This procedure was repeated for 1,000 iterations, and probabilities were determined as for the metameric vectors. Differences in vector magnitude, as measured by the corresponding eigenvalues, were similarly tested. Finally, relationships between molar form and size were explored through ANCOVA of form component (FPC) scores.

Visualization. Molar shape differences within and between species were visualized in *Morpheus* (Slice, 1998) by superimposition of wireframe representations of average molar shapes. Although less detailed than surface models, wireframe comparisons facilitate the identification of regional shape differences between groups. Shape variation patterns were also visualized using the Landmark morphing feature (Wiley et al., 2005). Three-dimensional morphs representing extremes of metameric and allometric shape variation were created by warping the atlas-molar surface to landmark configurations representing the average molar shape plus/minus a scaled coefficient vector (Dryden and Mardia, 1998). Vectors used were the metameric

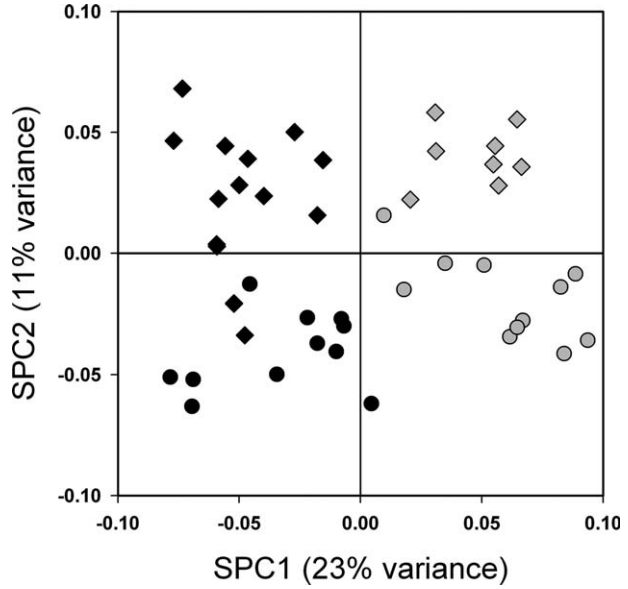

Fig. 2. Shape-space principal components analysis. The first principal shape component (SPC1) separates molars of *P. paniscus* (black) from those of *P. troglodytes* (gray); SPC2 separates M_1s (diamonds) from M_2s (circles).

regression coefficient vector and the FPC1 eigenvector (excluding the size coefficient; Mitteroecker et al., 2004). Just as bivariate regression coefficients express change in a dependent variable per unit change of the independent variable, the metameric and allometric coefficients summarize shape transformation at each landmark related to molar position and allometry, respectively. Corresponding (homologous) landmarks direct the warp, while thin-plate splines interpolate surface shape transformations between landmarks (Bookstein, 1991; Wiley et al., 2005).

RESULTS

Procrustes distances both within and between species were significant for all molar-shape comparisons. *Pan paniscus* showed the strongest shape disparity between M_1 and M_2 ($\rho = 0.0820$, $P < 0.001$) followed by *P. troglodytes* (0.0733, $P < 0.002$) and the M_1–M_2 distance calculated for all *Pan* (0.0691, $P < 0.001$). Interspecific distances calculated for M_1 and M_2 separately were similar ($\rho = 0.1092$ and 0.1048, respectively; both $P < 0.001$) and slightly greater than that calculated using a mixed-molar sample (0.0998, $P < 0.001$).

The first three principal shape components accounted for 44% of total molar shape variance. As seen in Fig. 2, SPC1 (23%) separates *P. paniscus* from *P. troglodytes* whereas SPC2 (11%) separates first and second molars. The third principal shape component (10%, not shown), weakly separates subspecies of *P. troglodytes*. The PCA ordination of specimens in form space is similar to that in shape space (Fig. 3a), with FPC1 (49% total variance) and FPC2 (7%) separating specimens by species and molar-row position, respectively. Higher order shape- and form-space components show no meaningful separation of specimens so were excluded from subsequent analyses.

Linear discriminant functions calculated on SPCs 1–3 classified molars with a high degree of accuracy as determined by leave-one-out cross-validation (Table 3). Using the pooled M_1–M_2 sample, 100% of *Pan* molars were accurately classified to species. Conversely, using the pooled *paniscus-troglodytes* sample, 95% of specimens were accurately classified to molar-row position. Two-way analysis of variance of SPC1 scores by species and wear yielded insignificant wear and interaction effects but a significant species effect ($F = 94.63$, $P < 0.0001$, excluding interaction). Excluding the interaction term, wear accounted for only 4% of explained variance in SPC1 versus 57% explained by species, thus ruling out differential wear as a meaningful contributor to interspecific molar shape differences. ANOVA of SPC2 scores by element and wear returned an insignificant interaction term but significant element and wear effects ($F = 69.64$, $P < 0.0001$; $F = 2.54$, $P < 0.04$, respectively, excluding interaction). Dropping the interaction term, wear accounted for 11% of explained variance in SPC2 versus 48% explained by molar-row position, making wear a secondary constituent of metameric shape difference.

Superimposition of average molar shapes (Figs. 4 and 5) highlights shape differences within and between species. In both chimpanzees and bonobos, the M_2 metaconid is more lingually positioned, the distal fovea is mesio distally compressed, and the crown walls, particularly below the protoconid, are less vertical than in M_1 (Fig. 4). In *P. paniscus* (Fig. 5), both M_1 and M_2 molar crowns taper distally and the talonids are narrower, whereas in *P. troglodytes*, mesial and distal crown breadths are more uniform, resulting in a more rectangular crown shape. In *P. troglodytes*, the metaconid is also more distal, the talonid is higher relative to the cemento-enamel junction, and the cusps are lower relative to the talonid (Fig. 5, right), yielding a more open basin and a relatively bunodont morphology.

Metameric Variation

Two-way ANOVA of SPC2 by species and molar-row position found no significant difference in metameric variation between *P. paniscus* and *P. troglodytes* (species-element interaction, $F = 0.75$, $P = 0.39$). Their metameric vectors differed by an angle of 61°; however, this difference was not statistically significant ($P = 0.297$). The vector-length difference between *P. paniscus* ($|\mathbf{M}| = 0.081$) and *P. troglodytes* ($|\mathbf{M}| = 0.073$) was likewise insignificant ($P = 0.368$), indicating that metameric shape differences in these species are of roughly equal magnitude. On the basis of these results, *P. paniscus* and *P. troglodytes* share a common pattern of metameric shape variation.

Visualization of the common metameric shape vector (Fig. 6) highlights differences between M_1 and M_2 in overall crown proportions, cusp size, and position similar to those observed in the direct shape comparisons (Fig. 4). Relative to that of M_1, the M_2 metaconid is expanded and its apex is more mesially and lingually positioned, resulting in buccolingual expansion of the mesial fovea. The M_2 entoconid, hypoconulid, and distal fovea are relatively smaller and the protoconid and hypoconid apices are relatively closer, resulting in mesiodistal

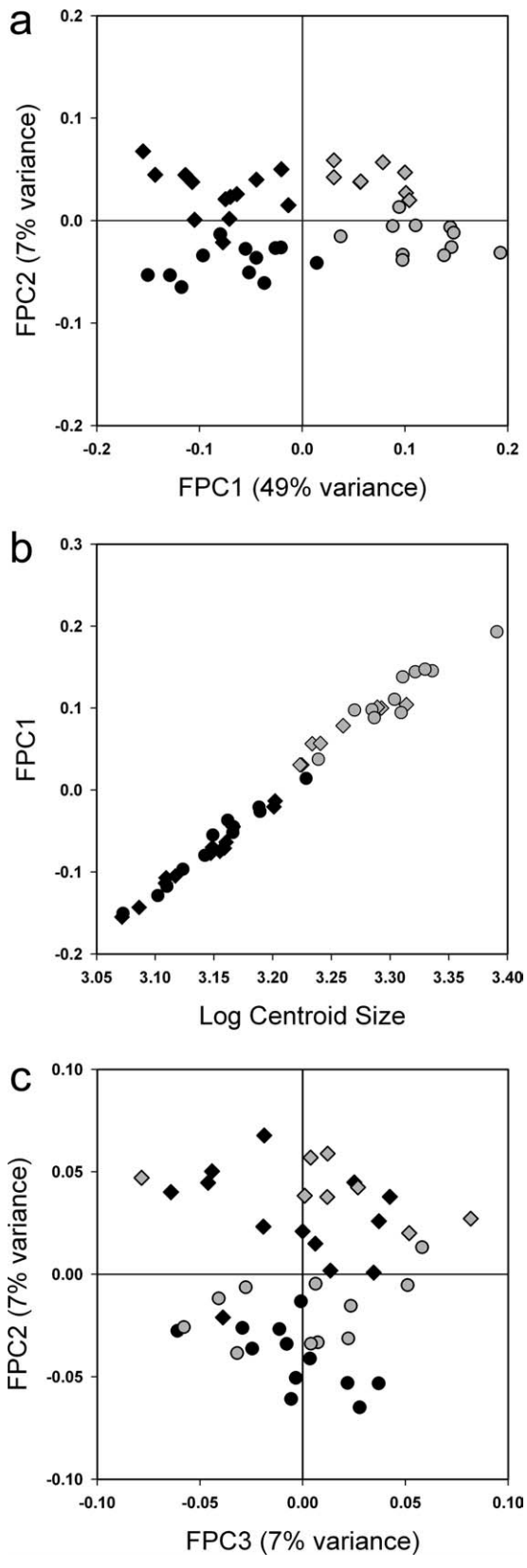

TABLE 3. Discriminant function classification results

Species classification	Ppn	Ptx
P. paniscus (N/%)	25/100	0/0
P. troglodytes (N/%)	0/0	19/100
Total error (%)	0	0
Molar classification	M_1	M_2
M_1 (N/%)	20/95	1/5
M_2 (N/%)	1/4	22/96
Total error (%)	5	5

Number (N) and percentage (%) of specimens classified to group using leave-one-out cross-validation.

compression of the talonid basin. The M_2 buccal wall, especially below the protoconid, is less vertical than that of M_1.

Allometric Variation

The first principal form component (Fig. 3a, FPC1) summarizes the common allometric shape trend and is, by design, strongly correlated with size ($r = 0.99$, $P < 0.001$). Plotting FPC1 against log centroid size (Fig. 3b) highlights the continuous distribution of specimens along the common allometric trajectory, which suggests that allometry is a major contributor to interspecific molar-shape differences. A subtle difference between species in the relationship of form to size is evidenced in Fig. 3b by the slightly steeper slope of *P. paniscus* (OLS slope of 1.09 vs. 0.96 for *P. troglodytes*), as well as in 3a, where the M_1 and M_2 clusters for the two species are slightly off-parallel.

Within species, first and second mandibular molars were found to have similar form-size relationships. Under ANCOVA of FPC1 scores, the molar-position and position-size interaction effects were insignificant in both *P. paniscus* (position: $F = 1.01$, $P = 0.33$; interaction: $F = 1.06$, $P = 0.31$) and *P. troglodytes* ($F = 0.80$, $P = 0.39$; $F = 0.81$, $P = 0.38$). Angular differences between M_1 and M_2 allometric vectors were insignificant in *P. paniscus* (34°, $P = 0.999$). In *P. troglodytes*, the vector angle was both large and statistically significant (107°, $P < 0.01$); however, this difference was attributable to the influence of a single M_1 outlier. Excluding this specimen, M_1 and M_2 allometric vectors were more similar and no longer significantly different (79°, $P = 0.07$).

Fig. 3. Form-space principal components analysis. (**a**) The first principal form component (FPC1), which summarizes both geometric size and the shared allometric shape trend, separates species of *Pan*; FPC2 separates first and second molars within species. (**b**) By design, FPC1 scores are linearly correlated with size ($r = 0.99$); the form-size plot highlights the nearly continuous distribution of molars along the common allometric trajectory. A subtle difference between species in the form-size relationship is manifest in the slightly steeper slope of *P. paniscus* (OLS slope of 1.09 vs. 0.96 for *P. troglodytes*), as well as in (a), where the M_1 and M_2 clusters of the two species are slightly off-parallel. (**c**) The plot of FPC2 against FPC3 rotates (a) by 90° to view the data cloud along the axis of allometry; with allometric shape visually subtracted, the species overlap extensively, demonstrating the absence of specific differences independent of size. Symbols follow Fig. 2.

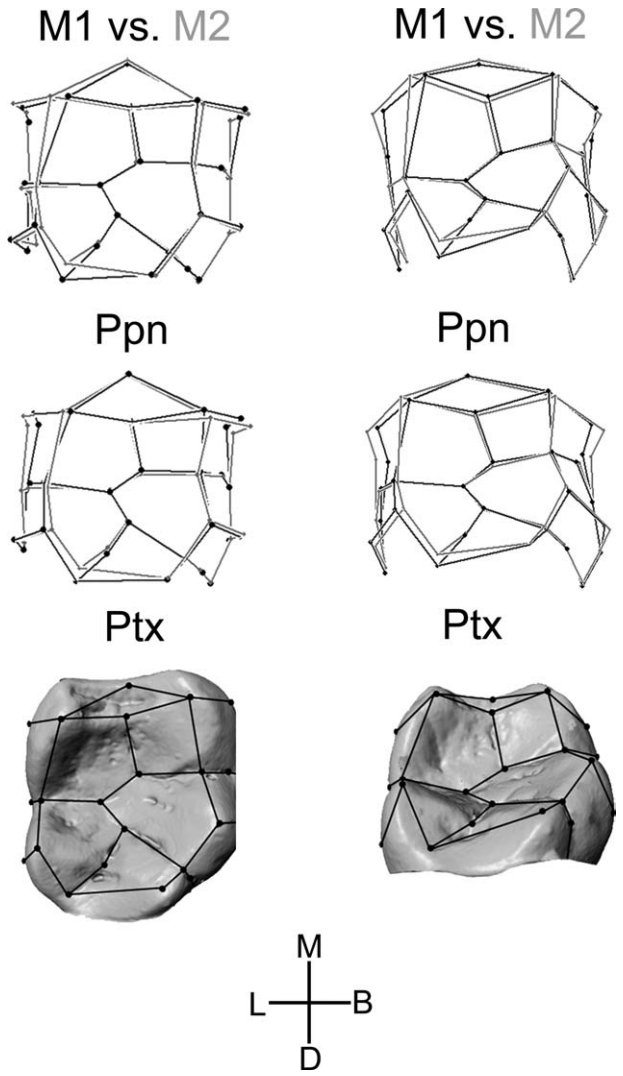

Fig. 4. Molar shape differences within species. Left column: occlusal view of superimposed average M_1 (black wireframe) and average M_2 (gray wireframe) for *P. paniscus* (Ppn, top) and *P. troglodytes* (Ptx, middle), respectively. Right column: same comparisons with the mesial crown elevated $\sim 45^\circ$ to demonstrate the absence of metameric differences in cusp relief or basin height relative to the cemento-enamel junction. All views are of right molars; mesial is toward figure top and buccal toward figure right.

Thus, for neither species was the null hypothesis of a shared allometric pattern conclusively rejected. Under ANCOVA of FPC1 by species and size, the slope difference apparent in Fig. 3b fell short of statistical significance (species-size interaction, $F = 3.78$, $P = 0.588$); however, the angular difference between the two species' allometric vectors was significant (42°, $P < 0.001$). The magnitude of within-species allometric variation, as measured by the first eigenvalue, also did not differ ($P = 0.894$). Visualization of the common allometric vector (Fig. 7) shows larger molars to have squarer crowns; lower cusp relief; broader, more open basins; relatively smaller metaconids and hypoconulids; and more peripheral buccal cusps, particularly the hypoconulid.

DISCUSSION

Three-dimensional geometric shape analysis has become a standard tool in the morphologist's kit; however, its potential has yet to be fully realized in the sphere of dental studies. Lavelle (1978) and Wood et al.'s (1983) early experiments with 2D Procrustes analysis of hominin molars demonstrated the method's promise, and Hartman's (1989) analysis of hominoid occlusal landmarks established the greater discriminatory power of 3D data. The high-resolution occlusal scans obtained by Ungar and colleagues (e.g., Ungar and Williamson, 2000) revealed the potential of laser digitization, but it is only with the advent of multi-axial, semi-automated laser scanning systems and comparable optical topometric systems that it has become economical to create statistically valid samples of anatomically accurate "virtual molars" (e.g., Ulhaas et al., 2004; King et al., 2005; Ulhaas et al., 2007). These developments, in tandem with advances in morphometric software (e.g., Landmark; Wiley et al., 2005), have enabled us to move beyond the essentially 2D approach of many recent studies (Martinón-Torres et al., 2006; Bailey and Wood, 2007; Gómez-Robles et al., 2007; Gómez-Robles et al., 2008; White, 2009) toward truly 3D analyses of molar shape deploying the full GM arsenal of direct shape comparison, multivariate statistical analysis, and computer graphic visualization (Skinner et al., 2008; Skinner et al., 2009a).

An additional obstacle to GM dental analysis is the relative scarcity of consistently identifiable, unambiguously homologous landmarks. Consequently, the landmark set used in this study is relatively sparse ($p = 29$) in comparison with cranial datasets, although denser than that of prior dental studies, which relied heavily on semi-landmarks (e.g., Olejniczak et al., 2004; Martinón-Torres et al., 2006; Bailey and Wood, 2007; Gómez-Robles et al., 2007, 2008; Skinner et al., 2008). Its discriminatory power thus speaks both to the substantial information content of hominid molars and the efficacy of Procrustes-based shape analysis.

Principal components analysis of molar shape (Fig. 2) separates molars by species (SPC1) and molar position (SPC2), and permutation of Procrustes distances confirms that shape differences summarized by these components are statistically significant. Linear discriminant functions calculated on SPCs 1–3 for the entire ($N = 44$) sample classify molars to species with 100% accuracy and to molar-row position with 95% accuracy. This compares favorably with Pilbrow's species-classification rates of 73–96% using 15 traditional measurements and with the results of Skinner et al. based on scores on 8–12 principal shape components (Pilbrow, 2006; Skinner et al., 2009a). Our findings simultaneously support Pilbrow's (2006, 2007) conclusion that hominid crown-shape variation is an appropriate basis for taxonomic classification and underscore the potential of geometric dental analysis. That 100% accuracy is possible even with relatively small samples suggests these methods are well suited for paleontological analyses, where inadequate reference samples are common.

On the basis of our results, metameric shape vectors of *P. paniscus* and *P. troglodytes* do not differ significantly in either orientation (angle) or magnitude (length). We cannot rule out the possibility that differences in metameric patterning are present but

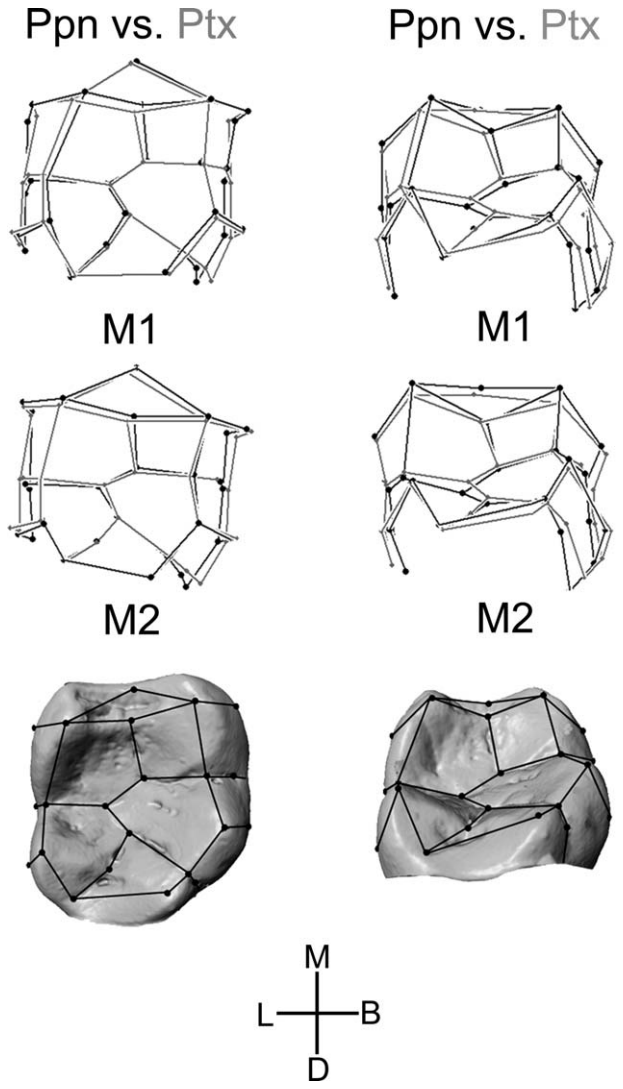

Fig. 5. Molar shape differences between species. Left column: occlusal view of superimposed M_1s and M_2s (top and middle, respectively) of *P. paniscus* (Ppn, black) and *P. troglodytes* (Ptx, gray). Right column: same comparisons with the mesial crown elevated $\sim 45^\circ$ to demonstrate species differences in cusp relief and basin height relative to the cemento-enamel junction. All views are of right molars oriented as in Fig. 4.

undetectable with our relatively small samples. However, the ability of the same samples to differentiate chimpanzee and bonobo allometric vectors argues against this possibility, as does the obvious similarity of their metameric shape trends (Fig. 4). In both species, M_2 is characterized by a mesio lingually expanded metaconid, expanded mesial fovea, proportionately reduced distal crown moiety, and more curved buccal crown wall. Although M_1s in our sample were, on average, more worn than M_2s, metameric differences in cusp relief were not observed. This supports the determination, based on ANOVA results, that differential wear is a relatively small constituent of metameric shape variation in this sample.

This study's findings are at odds with those of Skinner et al. (2009a), who reported that the M_2 mesial dentine horns in *Pan* are both lower and more centrally located that those of M_1. However, our findings match closely the shared metameric pattern described by Hlusko (2002) for *P. troglodytes*, *Gorilla*, and (to a lesser extent) South African australopiths. That this meristic pattern is also shared by *P. paniscus* makes it probable that it represents the ancestral hominid pattern. The apparent inconsistency between crown-surface shape and EDJ shape may arise from differences in wear pattern (as opposed to magnitude) or enamel distribution. This discrepancy merits further investigation, as it may have bearing on the difference in australopith M_1 and M_2 crown heights described by Skinner et al. (2008).

Mandibular-molar shape in *Pan* is strongly correlated with size. Within species, first and second molars have statistically indistinguishable allometric vectors. But due to the small samples available for these comparisons ($N \approx 10$ per species/molar partition), our conclusion that M_1 and M_2 share common scaling patterns within species must be considered preliminary. Chimpanzee and bonobo allometric vectors have equal magnitudes but significantly different vector orientations. Given the findings of Corruccini and McHenry (Corruccini and McHenry, 1979; McHenry and Corruccini, 1981), this result was not completely unexpected. The congruence of our results with these earlier results based on more traditional data makes it difficult to dismiss the significant difference in species allometric patterns as an artifact of sample size and/or composition.

By the strict criterion of shared static allometric vectors, molars of *P. paniscus* and *P. troglodytes* are not allometrically scaled. Nevertheless, the common allometric shape trend (Fig. 7) appears sufficient to explain most interspecific molar shape differences (Fig. 5). The relatively larger metaconid, broader mesial crown, greater cusp relief, and more lingual hypoconulid previously described for bonobos (McHenry and Corruccini, 1981; Kinzey, 1984; Uchida, 1996) are predicted by the visualization of the common allometric shape vector (Fig. 7). Furthermore, all *post hoc* attempts to identify size-independent species differences, through visualization of multiple regression coefficients, etc., were

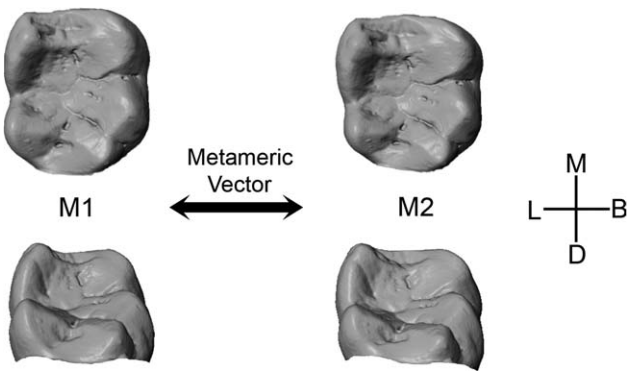

Fig. 6. Shape variation summarized by the common metameric shape vector. Morphs, shown in occlusal view (top) and with the mesial crown elevated as in Fig. 4 (bottom), represent extremes of shape variation along the common metameric vector, which summarizes differences between M_1 and M_2 in cusp size and position, basin proportions, and buccal crown-wall curvature. All views are of right molars.

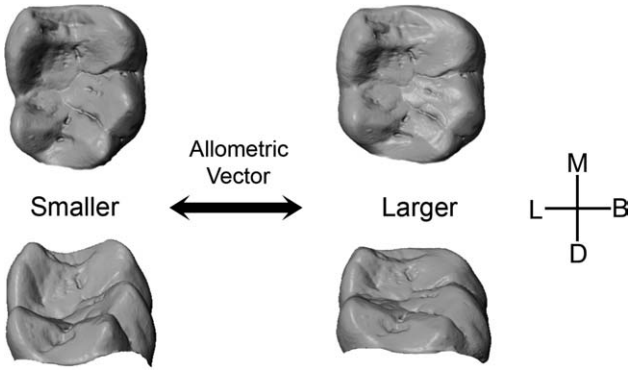

Fig. 7. Shape variation summarized by the common allometric shape vector. Morphs, oriented as in Fig. 6, represent extremes of shape variation along the common allometric vector, which summarizes differences in crown height and breadth, relative cusp size and relief, and buccal-cusp position. All views are of right molars.

completely unsuccessful. The apparent absence of size-independent differences is reflected in the lack of separation on higher order principal components in both shape- and form-space and is demonstrated graphically by Fig. 3c where, viewed parallel to the axis of shared allometry, species are indistinguishable. Thus, it would seem that Pilbrow's "size-corrected" shape variables discriminated between species precisely because they did not correct for allometry.

Researchers who investigate biological shape variation in differently sized phena, whether species or sexes, must be ever watchful against attributing spurious size-shape correlations to the effects of allometry. This is particularly true of pairwise comparisons because, as stated in Euclid's first postulate, any two points define a line (Weisstein, 2009). It is thus reasonable to ask whether the close correspondence between the species shape differences demonstrated in Fig. 5 and the allometric shape trend visualized in Fig. 7 is merely a statistical artifact. The nearly continuous distribution of specimens along the common allometric trajectory (Fig. 3a,b) argues against this interpretation. Further studies incorporating larger samples, particularly of subspecies of *P. troglodytes*, should settle this question conclusively.

In light of our present results, we conclude that Kinzey's statement, "the suggestion of Gould (1975) and others that the pygmy chimpanzee is merely a scaled-down model of the common chimpanzee is not reflected in the dental data" (1984: 83), is valid only in the narrow sense that species allometric vectors are statistically distinguishable. However, this appears to be a distinction with no practical consequence. Residual shape differences not accounted for by the common allometric trend are so minor as to be undiscernable, reminding us that statistical significance and biological significance can be different things entirely.

Many of the molar shape characteristics and variation patterns observed in this study have been described previously (Corruccini and McHenry, 1979; McHenry and Corruccini, 1981; Kinzey, 1984; Uchida, 1996; Hlusko, 2002; Pilbrow, 2006), but not all findings concur with previous studies. Direct comparisons of bonobo and chimpanzee molar shape (Fig. 5) show little indication of the "enlarged crown components, increased talonid height, and square shape of pygmy chimpanzee molars" described by Corruccini and McHenry (1979: 1342). In our comparisons, cusp proportions, excluding the metaconid, are generally similar in the two species, the bonobo talonid basin is lower relative to the cemento-enamel junction, and the chimpanzee molar is squarer.

These discrepancies may be attributable to methodological differences but should be investigated further, particularly with respect to functional morphology and dietary adaptation. The increased cusp relief and reciprocally deeper basins of bonobo molars (Fig. 5) increase their shearing capacity relative to that of chimpanzees (Kay, 1973; Kinzey, 1984). This functional difference is consistent with the bonobo's heavy reliance on terrestrial herbaceous vegetation (THV) as a fallback food during periods of fruit scarcity (Malenky and Wrangham, 1994; Conklin-Brittain et al., 2001, 2006). Chimpanzees, by contrast, do not increase foliage consumption to nearly the same extent but disperse to search for fruit instead (Conklin-Brittain et al., 2001). This divergence in fallback strategies raises an interesting point. If increased cusp relief is an allometric correlate of reduced molar size (Fig. 7) rather than the result of direct selection for increased shearing capacity, the bonobo's ability to rely upon THV as a seasonal fallback food (Malenky and Wrangham, 1994; Conklin-Brittain et al., 2001) could be a co-optation in the sense of Gould and Vrba (1982). Then again, *Gorilla* possesses the largest molars, highest cusp relief, and greatest relative shearing capacity of any extant hominid (Kay and Ungar, 1997), so the relationship between cusp relief and molar size within and across hominid genera requires further investigation.

Whereas most prior studies have focused on allometric scaling of molar size, this study demonstrates that scaling of molar shape can be a major contributor to taxonomic differences in molar form. The extent to which the variation patterns observed here can be generalized to other hominids remains to be seen, but the implications for interpretation of molar shape variation in the fossil record are manifest. If, for example, the low cusp-relief of *Paranthropus* molars (Robinson, 1956; Skinner et al., 2008) can be explained by increased molar size without reference to direct selection on molar shape, our understanding of the forces driving early hominin morphological and ecological diversity may be altered. The questions raised by this study invite deeper scrutiny of the nature of hominid dental variation.

CONCLUSIONS

Three-dimensional geometric shape analysis is a powerful tool for the investigation of biological shape variation. In this study, we used a 3D digital morphometric analysis to investigate meristic and allometric shape variation in mandibular molars of *Pan*. Procrustes-based 3D shape variables classified molars to taxon and tooth-row position with considerable accuracy. Comparisons of metameric shape vectors showed chimpanzees and bonobos to share a common pattern of metameric shape variation that is probably primitive for hominids. In both species, M_2s are characterized by mesiolingual expansion of the metaconid and mesial fovea; reduction of the distal cusps and distal fovea; mesiodistal compression of the talonid basin; and increased curvature of the buccal crown wall. Within

species, M_1 and M_2 appear to have common allometric scaling patterns. Although species allometric vectors were found to be significantly different, the common allometric trend accounts for most shape differences between chimpanzee and bonobo mandibular molars. Established differences in cusp proportion and location, crown breadth, and cusp relief are predicted by the common allometric vector. When allometric effects are factored out, interspecific differences in molar shape are effectively eliminated. These findings have implications for our understanding of morphological and ecological diversity in *Pan* and suggest that further investigations into the nature of hominid molar shape variation are needed.

ACKNOWLEDGMENTS

For access to specimens and curatorial assistance, the authors thank O. Herschensohn (Peabody Museum of Archaeology and Ethnology, Harvard University), E. Gilissen and W. Wendelen (Royal Museum for Central Africa), G. Sawyer (American Museum of Natural History, Division of Anthropology), S. Bailey (Center for the Study of Human Origins, New York University), the late D. Swindler, and especially P. Ungar for consenting to their use of the bonobo dental molds. They are grateful for the diligence and dedication of their student research assistants, S. Cooke, L. Halenar, and S. Wong, and the technical assistance of E. Delson, J. Rohlf, D. Wiley, N. Amenta, W. Harcourt-Smith, K. St. John, D. Ghosh, K. McNulty, S. Frost, M. Giova, and M. Brennen. They thank J. Laitman and several anonymous reviewers for their helpful comments and corrections. Institutional and logistical support was provided by NYCEP/NYCEP Morphometrics Group, CUNY (Brooklyn College, Bronx Community College), Midwestern University, the Field Museum of Natural History, the American Museum of Natural History, and the University of Illinois–Urbana-Champaign. This paper is NYCEP Morphometrics Contribution #40.

LITERATURE CITED

Ackermann RR, Krovitz G. 2002. Common patterns of facial ontogeny in the hominid lineage. Anat Rec B New Anat 269:142–147.

Baab K, McNulty KP. 2009. Size, shape, and asymmetry in fossil hominins: the status of the LB1 cranium based on 3D morphometric analyses. J Hum Evol 57:608–622.

Bailey SE. 2008. Inter- and intra-specific variation in *Pan* tooth crown morphology: implications for Neandertal taxonomy. In: Irish JD, Nelson GC, editors. Technique and application in dental anthropology. Cambridge, UK: Cambridge University Press. p 293–316.

Bailey SE, Wood BA. 2007. Trends in postcanine occlusal morphology within the hominin clade: the case of *Paranthropus*. In: Bailey SE, Hublin J-J, editors. Dental perspectives on human evolution: state-of-the-art research in dental paleoanthropology. Dordrecht, The Netherlands: Springer. p 33–52.

Bateson W. 1894. Materials for the study of variation treated with especial regard to discontinuity in the origin of species. London: MacMillan.

Benefit BR. 1993. The permanent dentition and phylogenetic position of *Victoriapithecus* from Maboko Island, Kenya. J Hum Evol 25:83–172.

Berge C, Penin X. 2004. Ontogenetic allometry, heterochrony, and interspecific differences in the skull of African apes, using tridimensional Procrustes analysis. Am J Phys Anthropol 124:124–138.

Bookstein FL. 1991. Morphometric tools for landmark data: geometry and biology. Cambridge: Cambridge University Press.

Bookstein FL, Gunz P, Mitteroecker P, Prossinger H, Schaefer K, Seidler H. 2003. Cranial integration in *Homo*: singular warps analysis of the midsagittal plane in ontogeny and evolution. J Hum Evol 44:167–187.

Bookstein FL, Schaefer K, Prossinger H, Seidler H, Fieder M, Stringer C, Weber G, Arsuaga J-L, Slice DE, Rohlf J, Recheis W, Mariam AJ, Marcus LF. 1999. Comparing frontal cranial profiles in archaic and modern *Homo* by morphometric analysis. Anat Rec 257:217–224.

Boughner JC, Dean CM. 2004. Does space in the jaw influence the timing of molar crown initiation? A model using baboons (*Papio anubis*) and great apes (*Pan troglodytes*, *Pan paniscus*). J Hum Evol 46:255–277.

Braga J, Thackeray FJ. 2003. Early *Homo* at Kromdraai B: probabilistic and morphological analysis of the lower dentition. C R Palevol 2:269–279.

Brunet M, Beauvilain A, Coppens Y, Heintz E, Moutaye AHE, Pilbeam D. 1996. *Australopithecus bahrelghazali*, une nouvelle espèce d'Hominidé ancien de la région de Koro Toro (Tchad). CR Acad Sci Ser IIa 322:907–913.

Cobb SN, O'Higgins P. 2007. The ontogeny of sexual dimorphism in the facial skeleton of African apes. J Hum Evol 53:176–190.

Collyer ML, Adams DC. 2007. Analysis of two-state multivariate phenotypic change in ecological studies. Ecology 88:683–692.

Conklin-Brittain NL, Knott CD, Wrangham RW. 2001. The feeding ecology of apes. In: Apes: challenges for the 21st Century. Brookfield, IL: Chicago Zoological Society. p 167–174.

Conklin-Brittain NL, Knott CD, Wrangham RW. 2006. Energy intake by wild chimpanzees and orangutans: methodological considerations and a preliminary comparison. In: Hohmann G, Robbins MM, Boesche C, editors. Feeding ecology in apes and other primates: ecological, physiological, and behavioural aspects. Cambridge: Cambridge University Press. p 445–472.

Coolidge HJ, Jr. 1933. *Pan paniscus*. Pigmy chimpanzee from south of the Congo river. Am J Phys Anthropol 18:1–59.

Corruccini RS, McHenry HM. 1979. Morphological affinities of *Pan paniscus*. Science 204:1341–1343.

Delson E, Harvati K, Reddy D, Marcus LF, Mowbray K, Sawyer GJ, Jacob T, Marquez S. 2001. The Sambungmacan 3 *Homo erectus* calvaria: a comparative morphometric and morphological analysis. Anat Rec 262:389–397.

Dryden IL, Mardia KV. 1998. Statistical shape analysis. New York: John Wiley.

Gómez-Robles A, Martinón-Torres M, Bermúdez de Castro JM, Margvelashvili A, Bastir M, Arsuaga JL, Pérez-Pérez A, Estebaranz F, Martínez LM. 2007. A geometric morphometric analysis of hominin upper first molar shape. J Hum Evol 53:272–285.

Gómez-Robles A, Martinón-Torres M, Bermúdez de Castro JM, Prado L, Sarmiento S, Arsuaga JL. 2008. Geometric morphometric analysis of the crown morphology of the lower first premolar of hominins, with special attention to Pleistocene *Homo*. J Hum Evol 55:627–638.

Good PI. 2000. Permutation tests: a practical guide to resampling methods for testing hypotheses. New York: Springer.

Goodnight JH. 1978. Tests of hypotheses in fixed effects linear models. SAS Technical Report R-101. Cary, NC: SAS Institute, Inc.

Gould SJ. 1975. Allometry in primates, with emphasis on scaling and the evolution of the brain. Contrib Primatol 5:244–292.

Gould SJ, Vrba ES. 1982. Exaptation—a missing term in the science of form. Paleobiology 8:4–15.

Gower JC. 1975. Generalized Procrustes analysis. Psychometrika 40:33–55.

Gunz P. 2005. Statistical and geometric reconstruction of hominid crania: reconstructing australopithecine ontogeny. PhD dissertation. University of Vienna.

Gunz P, Mitteroecker P, Neubauer S, Weber GW, Bookstein FL. 2009. Principles for the virtual reconstruction of hominin crania. J Hum Evol 57:48–62.

Hartman SE. 1989. Stereophotogrammetric analysis of occlusal morphology of extant hominoid molars. Am J Phys Anthropol 80:145–166.

Harvati K. 2004. 3-D geometric morphometric analysis of temporal bone landmarks in Neandertals and modern humans. In: Elewa AMT, editor. Morphometrics—applications in biology and paleontology. New York: Springer. p 245–258.

Harvati K, Frost SR, McNulty KP. 2004. Neanderthal taxonomy reconsidered: implications of 3D primate models of intra- and interspecific differences. Proc Natl Acad Sci USA 101:1147–1152.

Hlusko LJ. 2002. Identifying metameric variation in extant hominoid and fossil hominid mandibular molars. Am J Phys Anthropol 118:86–97.

Johanson DC. 1974a. An odontological study of the chimpanzee with some implications for hominoid evolution. PhD dissertation. University of Chicago.

Johanson DC. 1974b. Some metric aspects of the permanent and deciduous dentition of the pygmy chimpanzee (*Pan paniscus*). Am J Phys Anthropol 41:39–48.

Johanson DC, Lovejoy CO, Kimbel WH, White TD, Ward SC, Bush ME, Latimer BE, Coppens Y. 1982. Morphology of the Pliocene partial hominid skeleton (A.L. 288-1) from the Hadar Formation, Ethiopia. Am J Phys Anthropol 57:403–452.

Jolicoeur P. 1963. The multivariate generalization of the allometry equation. Biometrics 19:497–499.

Jolicoeur P, Mosimann JE. 1960. Size and shape variation in the painted turtle, a principal component analysis. Growth 24:339–354.

Kay RF. 1973. Mastication, molar tooth structure and diet in primates. PhD dissertation. Duke University.

Kay RF, Ungar PS. 1997. The dietary adaptations of European Miocene catarrhines. Proc Natl Acad Sci USA 92:5479–5481.

King RL, Rosenberger AL, Kanda LL. 2005. Artificial neural networks and three-dimensional digital morphology: a pilot study. Folia Primatol 76:303–324.

Kinzey WG. 1984. The dentition of the pygmy chimpanzee, *Pan paniscus*. In: Susman RL, editor. The pygmy chimpanzee: evolutionary biology and behavior. New York: Plenum Press. p 65–88.

Klingenberg CP. 1996. Multivariate allometry. In: Marcus LF, Corti M, Loy A, Naylor GJP, Slice DE, editors. Advances in morphometrics. New York: Plenum.

Lavelle CLB. 1978. An analysis of molar tooth form. Acta Anat 100:282–288.

Leakey MG, Feibel CS, McDougall I, Walker A. 1995. New four-million-year-old hominid species from Kanapoi and Allia Bay, Kenya. Nature 376:535–571.

Leakey MG, Feibel CS, McDougall I, Ward CV, Walker A. 1998. New specimens and confirmation of an early age for *Australopithecus anamensis*. Nature 393:62–66.

Leakey MG, Hay RL, Curtis GH, Drake RE, Jackes MK, White TD. 1976. Fossil hominids from the Laetolil Beds. Nature 262:460–466.

Levene H. 1960. Robust tests for the equality of variance. In: Olkin I, editor. Contributions to probability and statistics. Palo Alto, CA: Stanford University Press. p 278–292.

Lockwood CA, Kimbel WH, Lynch JM. 2004. Morphometrics and hominoid phylogeny: support for a chimpanzee-human clade and differentiation among great ape species. Proc Natl Acad Sci USA 101:4356–4360.

Lockwood CA, Lynch JM, Kimbel WH. 2002. Quantifying temporal bone morphology of great apes and humans: an approach using geometric morphometrics. J Anat 201:447–464.

Malenky RK, Wrangham RW. 1994. A quantitative comparison of terrestrial herbaceous food consumption by *Pan paniscus* in the Lomako Forest, Zaire, and *Pan troglodytes* in the Kibale Forest, Uganda. Am J Primatol 32:1–12.

Martinón-Torres M, Bastir M, Bermúdez de Castro JM, Gómez A, Sarmiento S, Muela A, Arsuaga JL. 2006. Hominin lower second premolar morphology: evolutionary inferences through geometric morphometric analysis. J Hum Evol 50:523–533.

McHenry HM, Corruccini RS. 1980. Late tertiary hominoids and hominid origins. Nature 285:297–298.

McHenry HM, Corruccini RS. 1981. *Pan paniscus* and human evolution. Am J Phys Anthropol 54:355–367.

McNulty KP. 2005a. Permutation_procd.txt, updated: December 7, 2007. In: SAS for Morphometrics. Available at: http://anthropology.umn.edu/labs/eal/sas/Permutation_procd.txt. Accessed October 27, 2010.

McNulty KP. 2005b. Procrustes_distance.txt, updated: December 7, 2007. In: SAS for Morphometrics. Available at: http://anthropology.umn.edu/labs/eal/sas/Procrustes_distance.txt. Accessed October 27, 2010.

McNulty KP, Radulesco C, Samson P, Feru M, Delson E. 1999. Morphology and identification of a previously undescribed fossil catarrhine tooth from the middle Miocene of Romania. Am J Phys Anthropol Suppl 28:199.

Mitteroecker P, Gunz P, Bernhard M, Schaefer K, Bookstein FL. 2004. Comparison of cranial ontogenetic trajectories among great apes and humans. J Hum Evol 46:679–698.

Mosimann JE, Malley JD. 1979. Size and shape variables. In: Orioci L, Rao CR, Stiteler WM, editors. Multivariate methods in ecological work. Fairland, MD: International Co-Operative Publishing House. p 175–189.

Olejniczak A, Martin L, Ulhaas L. 2004. Quantification of dentine shape in anthropoid primates. Ann Anat 186:479–485.

Pilbrow VC. 2006. Population systematics of chimpanzees using molar morphometrics. J Hum Evol 51:646–662.

Pilbrow VC. 2007. Patterns of molar variation in great apes and their implications for hominin taxonomy. In: Bailey SE, Hublin J-J, editors. Dental perspectives on human evolution: state-of-the-art research in dental paleoanthropology. Dordrecht, The Netherlands: Springer. p 9–32.

Polly PD, Head JJ. 2004. Maximum-likelihood identification of fossils: taxonomic identification of Quaternary marmots (Rodentia, Mammalia) and identification of vertebral position in the pipesnake *Cylindrophis* (Serpentes, Reptilia). In: Elewa AMT, editor. Morphometrics—applications in biology and paleontology. New York: Springer. p 197–221.

Ponce de Leon M, Zollikover CPE. 2001. Neandertal cranial ontogeny and its implications for late hominid diversity. Nature 412:534–537.

Remane A. 1962. Masse und proportionen des Milchgebisses der Hominoidea. Bibl Primatol 1:229–238.

Robinson C. 2003. Extant hominoid and australopith mandibular morpohology: assessing alpha taxonomy and phylogeny using mandibular characters. PhD dissertation. New York University.

Robinson JT. 1956. The dentition of the Australopithecinae. Transv Mus Mem 9.

Rohlf FJ, Slice DE. 1990. Methods for comparison of sets of landmarks. Syst Zool 29:40–59.

SAS. 1990. SAS/STAT User's Guide, Version 6, 4th ed., Vol. 1. Cary, NC: SAS Institute, Inc.

Scott JE, Lockwood CA. 2004. Patterns of tooth crown size and shape variation in great apes and humans and species recognition in the fossil record. Am J Phys Anthropol 125:303–319.

Shea BT. 1982. Growth and size allometry in the African Pongidae: cranial and postcranial analyses. PhD dissertation. Duke University.

Skinner MM, Gunz P, Wood BA, Boesch C. 2009a. Discrimination of extant *Pan* species and subspecies using the enamel-dentine junction morphology of lower molars. Am J Phys Anthropol 140:234–243.

Skinner MM, Gunz P, Wood BA, Hublin J-J. 2008. Enamel-dentine junction (EDJ) morphology distinguishes the lower molars of *Australopithecus africanus* and *Paranthropus robustus*. J Hum Evol 55:979–988.

Skinner MM, Wood BA, Hublin J-J. 2009b. Protostylid expression at the enamel-dentine junction and enamel surface of mandibular molars of *Paranthropus robustus* and *Australopithecus africanus*. J Hum Evol 56:76–85.

Slice DE. 1998. Morpheus et al.: software for morphometric research. 01-30-98. Stony Brook, NY: Stony Brook University.

Slice DE. 2007. Geometric morphometrics. Ann Rev Anthropol 36:261–281.

Slice DE, Bookstein FL, Marcus LF, Rohlf FJ. 1996. Appendix I—a glossary for geometric morphometrics. In: Marcus LF, Corti M, Loy A, Naylor GJP, Slice DE, editors. Advances in morphometrics. New York: Plenum Press. p 531–551.

Suwa G, Kono RT, Katoh S, Asfaw B, Beyene Y. 2007. A new species of great ape from the late Miocene of Ethiopia. Nature 448:921–924.

Suwa G, White TD, Howell FC. 1996. Mandibular postcanine dentition from the Shungura Formation, Ethiopia: crown morphology, taxonomic allocation, and Plio-Pleistocene hominid evolution. Am J Phys Anthropol 101:247–282.

Swindler DR, Gavan JA, Turner WM. 1963. Molar tooth size variability in African monkeys. Hum Biol 35:104–122.

Uchida A. 1996. Craniodental variation among the great apes. Cambridge, MA: Peabody Museum of Archaeology and Ethnology.

Ulhaas L, Kullmer O, Schrenk F. 2007. Tooth wear and diversity in early hominid molars: a case study. In: Bailey SE, Hublin J-J, editors. Dental perspectives on human evolution: state-of-the-art research in paleoanthropology. Dordrecht, The Netherlands: Springer. p 369–390.

Ulhaas L, Kullmer O, Schrenk F, Henke W. 2004. A new 3-d approach to determine functional morphology of cercopithecoid molars. Ann Anat 186:487–493.

Ungar PS. 1996. Dental microwear of European Miocene catarrhines: evidence for diets and tooth use. J Hum Evol 31:335–366.

Ungar PS, Walker AC, Coffing K. 1994. Reanalysis of the Lukeino molar (KNM-LU 335). Am J Phys Anthropol 94:165–173.

Ungar PS, Williamson M. 2000. Exploring the effects of tooth wear on functional morphology: a preliminary study using dental topographic analysis. In: Paleontol Electr. Available at: http://palaeo-electronica.org/2000_1/gorilla/issue1_00.htm. Accessed January 20, 2009.

Weisstein EW. 2009. Euclid's postulates. In: MathWorld—A Wolfram Web Resource. Available at: http://mathworld.wolfram.com/EuclidsPostulates.html. Accessed May 19, 2009.

White J. 2009. Geometric morphometric investigation of molar shape diversity in modern lemurs and lorises. Anat Rec 292:701–719.

White TD, Johanson DC, Kimbel WH. 1981. *Australopithecus africanus*: its phyletic position reconsidered. S Afr J Sci 77:445–470.

Wiley DF, Amenta N, Alcantara DA, Ghosh D, Kil YJ, Delson E, Harcourt-Smith W, Rohlf FJ, St. John K, Hamann B. 2005. Evolutionary morphing. Proc IEEE Visualiz 2005.

Wood BA, Abbott SA, Graham SH. 1983. Analysis of the dental morphology of Plio-Pleistocene hominids II. Mandibular molars—study of cusp areas, fissure pattern and cross sectional shape of the crown. J Anat 137:287–315.

Zelditch ML, Swiderski DL, Sheets HD, Fink WL. 2004. Geometric morphometrics for biologists: a primer. New York: Elsevier Academic Press.